Advances in Mechanical and Materials Engineering

Volume 41, 2024, Pages 47-55
https://doi.org/10.7862/rm.2024.5

THE FACULTY OF MECHANICAL ENGINEERING AND AERONAUTICS
RZESZOW UNIVERSITY OF TECHNOLOGY

Original Research

Assessment of the Depth of the Plastically Deformed Top Layer in Burnishing Process of Shaft Using a Ceramic Tool

Piotr Paszta [1]*, Leszek Chałko [2], Rafał Kowalik [3]

[1] Faculty of Mechanical Engineering and Computer Science, Czestochowa University of Technology, al. Armii Krajowej 21, 42-201 Częstochowa, Poland
[2] Faculty of Mechanical Engineering, Casimir Pulaski Radom University, ul. Stasieckiego 54, 26-600 Radom, Poland; leszek.chalko@uthrad.pl
[3] Institute of Technical Sciences and Aeronautics, The University College of Applied Sciences in Chełm, ul. Pocztowa 54, 22-100 Chełm, Poland; rk16410@nauka.panschelm.edu.pl

* Correspondence: piotr.paszta@pcz.pl, tel.: +48 34 3250559

Received: 23 January 2024 / Accepted: 26 February 2024 / Published online: 5 March 2024

Abstract

Burnishing is one of the most effective methods of improving the strength of the surface layer of shafts as a result of strain strengthening of the material. This article presents an analytical approach to determining the the depth of the plastically deformed top layer of shaft based on Belyaev's theory. Contact of two bodies with an asymmetric stress state was assumed. A classic (symmetrical) solution was also considered. The aim of the research was to compare the calculated values of the depth of the plastically deformed top layer determined using these two methods. The calculations considered burnishing of shafts with a diameter of 48 mm made of steel with a yield stress of R_e = 450 MPa and R_e = 900 MPa. A burnishing tool with a Si_3N_4 ceramic tip was used for burnishing. It was found that in the range of low contact forces, the calculated values of the depth of the plastically deformed top layer using the asymmetric solution and the classical method are similar. It was also found that the relationship between the depth of the plastically deformed top layer and the contact force can be explained by a power equation with an accuracy of $R^2 > 0.999$.

Keywords: burnishing, plastically deformed layer, Belyaev's theory, shafts

1. Introduction

Burnishing involves applying pressure to the surface of the workpiece with a smooth and hard burnishing element (Zaleski, 2018). Burnishing using mechanical methods uses the pressure of a tool (pressure burnishing) or the kinetic energy of the tool or free particles (impact burnishing) (Czechowski and Kalisz, 2015; Skoczylas & Zaleski, 2022). This process is characterized by high efficiency in smoothing the surface of the workpiece and processing without the need to cool the burnished zone (Dobrzyński et al., 2019; Przybylski, 2016). Burnishing treatment is a technologically and economically effective method of producing the surface layers of machine parts (Kaldunski et al, 2019). In some cases, burnishing can replace the need for heat treatment of large elements (Kułakowska et al., 2014). Smooth burnishing is used to reduce the average surface roughness to approximately Ra = 0.05–0.10 μm (Czechowski & Toboła, 2017). The strengthening treatment is intended to ensure the required properties of the surface layer. Surface burnishing can produce a specific texture (up to a depth of several millimetres) and introduce compressive stresses up to approximately –1200 MPa (Przybylski, 1987). The beneficial effects of burnishing treatment include: increasing the hardness of the material, improving fatigue life, increasing resistance to abrasion and surface corrosion (Sachin et al., 2021; Zaleski & Skoczylas, 2019). Burnishing can be used to process internal and external surfaces, e.g. holes, cylinders, cones, shafts, as well as flat surfaces (Chodor & Kukielka, 2014; Dyl, 2011). Some burnishing methods can be used to create lubricating microgrooves on the mating

surfaces of bearing journals and bearing sleeves in order to increase the wear resistance of the mating elements (Patyk et al., 2017).

An analysis of contemporary work related to burnishing process shows that this technology is constantly being developed. Patyk et al. (2017) investigated the influence of burnishing depth on the surface roughness of shafts made of C45 steel. It was found that there is a burnishing depth value beyond which the surface roughness parameters will begin to increase, which is associated with the formation of flashes on the surface or the occurrence of local damage to the surface layer in the so-called Belyaev's points. Studies on burnishing of C45 steel shafts have shown that the greatest strengthening effect can be obtained after burnishing and subsequent hardening (Dyl, 2010). The opportunity of using SiC ceramic as a burnishing tool was investigated by Gałda and Pająk (2022). Dzierwa et al. (2020) analysed the effect of slide burnishing process on friction and wear of steel elements. The results of experiments proved the beneficial effect of the slide burnishing process on the reduction of volumetric wear.

In the exploitation of machines and devices, the issue of contact between two bodies occurs both when the tool comes into contact with the workpiece and when two cooperating parts come into contact. In both cases, surface pressures occur, which influence the value of elastic and plastic deformations. To determine the depth of the plastically deformed top layer in the process of surface burnishing with a ceramic tool, the description of the state of elastic stresses in contact between two bodies according to the Huber's hypothesis (Huber, 1904) can be used. Jezierski and Mazur (2002) developed the model of plasticised zone in the surface burnishing process based on the Huber's hypothesis of plastic deformation. Determining the depth of a plastically deformed layer using analytical methods is difficult. This article presents an analytical model for determining the depth of the plastically deformed top layer in the burnishing process.

2. Analytical analysis

2.1. Assumptions

The analysis of the burnishing process, the aim of which was to determine the thickness of the plastically deformed layer, was carried out using a Nklh2525 ball burnisher with a hydraulic presser (Fig. 1). The burnishing element was a bearing ball made of Si_3N_4 technical ceramics with a diameter of 6.25 mm. Ceramics as a tool material is used in machine technology in both machining and sliding burnishing. Steel shafts with the following material yield strengths of R_e = 450 MPa and R_e = 900 MPa were burnished. The hardness of the shaft material was 23 and 56 HRC. The diameter of the shafts was 48 mm. In all analyses, the tool pressure force was 200 N.

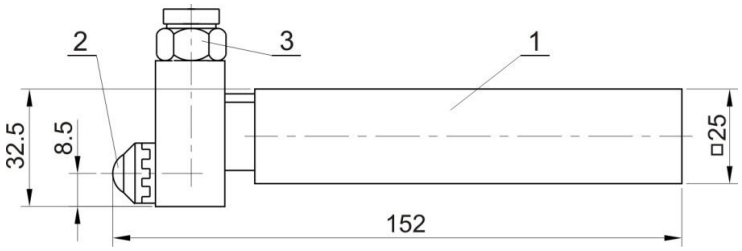

Fig. 1. The Nklh2525 ball burnisher with hydraulic presser: 1 – shank, 2 – ceramic ball, 3 – oil supply (Przybylski, 2004).

2.2. State of stress in contact between two bodies

The general formulas for describing the state of elastic stresses in contact between two bodies (Fig. 2) along the line of action of the contact force according to Belyaev's theory have the form (1)-(3) (Belyaev, 1957).

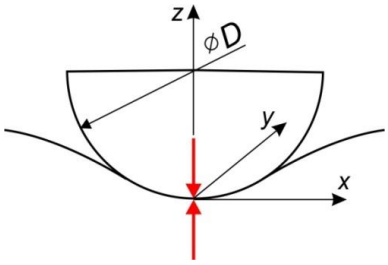

Fig. 2. Contact between two bodies in the *x*, *y*, *z* coordinate system.

$$\sigma_x = \frac{3F}{4\pi} 2z(1-\nu) \int_{z^2}^{\infty} \frac{ds}{(a^2+s)\sqrt{s(a^2+s)(b^2+s)}} - \frac{3F}{4\pi} 2z\nu \int_{z^2}^{\infty} \frac{ds}{s\sqrt{s(a^2+s)(b^2+s)}} - \frac{3F}{4\pi}(1-2\nu) \int_{z^2}^{\infty} \frac{ds}{(a^2+s)\sqrt{(a^2+s)(b^2+s)}} \tag{1}$$

$$\sigma_y = \frac{3F}{4\pi} 2z(1-\nu) \int_{z^2}^{\infty} \frac{ds}{(b^2+s)\sqrt{s(a^2+s)(b^2+s)}} - \frac{3F}{4\pi} 2z\nu \int_{z^2}^{\infty} \frac{ds}{s\sqrt{s(a^2+s)(b^2+s)}} + \frac{3F}{4\pi}(1-2\nu) \int_{z^2}^{\infty} \frac{ds}{(b^2+s)\sqrt{(a^2+s)(b^2+s)}} \tag{2}$$

$$\sigma_z = \frac{3F}{2\pi} \frac{1}{\sqrt{(a^2+z^2)(b^2+z^2)}} \tag{3}$$

where F is feed force of the tool to the workpiece; s is contact surface area of the tool and the workpiece; a and b are the minor and major semi-axis of the contact ellipse of the tool and the workpiece along the x and y axes, respectively; ν is Poisson's ratio; z is coordinate determining the depth of occurrence elastic stresses σ_x, σ_y and σ_z on the line of action of the feed force.
After solving the integrals in Eqs. (1) and (2) for $b > a$ (Ryzyk & Gradsztejn, 1964), the relationships (1)-(3) take the form:

$$\sigma_x = \frac{3F}{4\pi} 2z(1-\nu) \left[\frac{2b}{(b^2-a^2)} E(\varphi,k) - \frac{2}{b(b^2-a^2)} F(\varphi,k) - \frac{2z}{a^2} \frac{1}{\sqrt{(b^2+z^2)(a^2+z^2)}} \right] + \frac{3F}{4\pi} 2z\nu \left[\frac{2}{a^2 z} \sqrt{\frac{a^2+z^2}{b^2+z^2}} - \frac{2}{a^2 b} E(\varphi,k) \right] - \frac{3F}{4\pi}(1-2\nu) \frac{2}{a^2-b^2} \left(1 - \sqrt{\frac{b^2+z^2}{a^2+z^2}} \right) \tag{4}$$

$$\sigma_y = \frac{3F}{4\pi} 2z(1-\nu) \frac{2}{b(b^2-a^2)} [F(\varphi,k) - E(\varphi,k)] - \frac{3F}{4\pi} 2z\nu \left[\frac{2}{a^2 z} \sqrt{\frac{a^2+z^2}{b^2+z^2}} - \frac{2}{a^2 b} E(\varphi,k) \right] + \frac{3F}{4\pi}(1-2\nu) \frac{2}{b^2-a^2} \left(1 - \sqrt{\frac{a^2+z^2}{b^2+z^2}} \right) \tag{5}$$

$$\sigma_z = -\frac{3F}{2\pi} \frac{1}{\sqrt{(a^2+z^2)(b^2+z^2)}} \tag{6}$$

$$\varphi = arcsin \sqrt{\frac{b^2}{b^2+z^2}} = arcctg \frac{z}{g} \tag{7}$$

$$k = \sqrt{\frac{b^2-a^2}{b^2}} \text{ for } b > a \tag{8}$$

where $E(\varphi, k)$ is an elliptic integral of the second order:

$$E(\varphi,k) = \int_0^{\varphi} \sqrt{1 - k^2 sin^2\varphi} d\varphi \tag{9}$$

and $F(\varphi, k)$ is an elliptic integral of the first order:

$$F(\varphi,k) = \int_0^{\varphi} \frac{d\varphi}{\sqrt{1 - k^2 sin^2\varphi}} \tag{10}$$

To solve the problem of the thickness of the plastically deformed layer, the Huber-Mises-Hencky yield criterion according to Eq. (11) and integral tables (Ryzyk & Gradsztejn, 1964) should be used.

$$\sigma_{red} = \sqrt{\frac{1}{2}(\sigma_x - \sigma_v)^2 + (\sigma_v - \sigma_z)^2 + (\sigma_z - \sigma_x)^2} \tag{11}$$

where σ_{red} is equivalent stress; σ_1, σ_2 and σ_3 are principal stresses.

3.2. Thickness of plastically deformed layer

Based on the work by Mazur (2003), a short description of the theoretical solution for the thickness of a plastically deformed layer in contact between two bodies is presented. In equations (4)–(6) given in the section 3.1, the elliptic functions $E(\varphi, k)$ and $F(\varphi, k)$ can be expanded in series for calculations. Finishing their expansion with the second term, we get:

$$E(\varphi,k) = arcctg\frac{z}{b}\left(1 - \frac{1}{4}k^2 - \frac{3}{64}k^4\right) + \frac{z}{b}\frac{1}{1+\left(\frac{z}{b}\right)^2}\left[\frac{1}{4}k^2 + \frac{3}{64}k^4 + \frac{1}{32}k^4\frac{1}{1+\left(\frac{z}{b}\right)^2}\right] \tag{12}$$

$$F(\varphi,k) = arcctg\frac{z}{b}\left(1 + \frac{1}{4}k^2 + \frac{9}{64}k^4\right) + \frac{z}{b}\frac{1}{1+\left(\frac{z}{b}\right)^2}\left[\frac{1}{4}k^2 + \frac{9}{64}k^4 + \frac{3}{32}k^4\frac{1}{1+\left(\frac{z}{b}\right)^2}\right] \tag{13}$$

By grouping the appropriate expressions in the equations (4)–(6) and also introducing an auxiliary variable $w = \frac{a^2}{b^2} < 1$ and making appropriate transformations, we can obtain the final relationships for the stress components in the elastic zone at the contact of two bodies, which will be used to determine the feed force.

$$\sigma_x = \frac{3F}{\pi}\frac{1}{b^2(1-w)}\left[\frac{z}{b}\left(\frac{1-wv}{w}E(\varphi,k) - (1-v)F(\varphi,k)\right) + \frac{1-2v}{2}\left(1 - \sqrt{\frac{b^2+z^2}{b^2w+z^2}}\right) - \frac{1-w}{w}\frac{b^2wv+z^2}{\sqrt{(b^2w+z^2)(b^2+z^2)}}\right] \tag{14}$$

$$\sigma_y = \frac{3F}{\pi}\frac{1}{b^2(1-w)}\left[\frac{z}{b}\left(\frac{v-w}{w}E(\varphi,k) + (1-v)F(\varphi,k)\right) - \frac{2v-w}{2w}\sqrt{\frac{b^2w+z^2}{b^2+z^2}} - \frac{1-2v}{2}\right] \tag{15}$$

$$\sigma_z = \frac{3F}{\pi}\frac{1}{b^2(1-w)}\left[-\frac{b^2(1-w)}{2}\frac{1}{\sqrt{(b^2w+z^2)(b^2+z^2)}}\right] \tag{16}$$

where the functions $E(\varphi, k)$ and $F(\varphi, k)$ modify to the form:

$$E(\varphi,k)=arcctg\frac{z}{b}\left[1-\frac{1}{4}(1-w)-\frac{3}{64}(1-w)^2\right]+\frac{z}{b}\frac{1}{1+\left(\frac{z}{b}\right)^2}\left[\frac{1}{4}(1-w)+\frac{3}{64}(1-w)^2+\frac{1}{32}(1-w)^2\frac{1}{1+\left(\frac{z}{b}\right)^2}\right] \tag{17}$$

$$F(\varphi,k)=arcctg\frac{z}{b}\left[1-\frac{1}{4}(1-w)-\frac{9}{64}(1-w)^2\right]-\frac{z}{b}\frac{1}{1+\left(\frac{z}{b}\right)^2}\left[\frac{1}{4}(1-w)+\frac{9}{64}(1-w)^2+\frac{3}{32}(1-w)^2\frac{1}{1+\left(\frac{z}{b}\right)^2}\right] \tag{18}$$

where $k^2=1-w$.

Using the Huber-Mises-Hencky yield criterion and the derived equations (17) and (18), after transformations, we can obtain the relation (19) taking into account the thickness δ of the plastically deformed layer in a deformable body in contact with a non-deformable body.

$$\begin{aligned}F=\frac{\sqrt{2}}{3}\pi R_e b^2(1&-w)\left\{\left[\frac{\delta}{b}(1-\nu)\left(\frac{1+w}{w}E(\varphi,k)-2F(\varphi,k)\right)+1-2\nu\right.\right.\\&\left.-\frac{b^2w(1+w)(1-2\nu)-2\delta^2(\nu(1+w)-1)}{2w\sqrt{(b^2w+\delta^2)(b^2+\delta^2)}}\right]^2\\&+\left[\frac{\delta}{b}\left(\frac{\nu-w}{w}E(\varphi,k)+(1-\nu)F(\varphi,k)\right)-\frac{1-2\nu}{2}\right.\\&\left.+\frac{w(b^2+\delta^2)-2\nu(b^2w+\delta^2)}{2w\sqrt{(\delta^2w+\delta^2)(b^2+\delta^2)}}\right]^2\\&+\left[\frac{\delta}{b}\left(\frac{1-w\nu}{w}E(\varphi,k)-(1-\nu)F(\varphi,k)\right)+\frac{1-2\nu}{2}\right.\\&\left.\left.+\frac{b^2w^2(2\nu-1)+\delta^2(2(w\nu-1)+w)}{2w\sqrt{(b^2w+\delta^2)(b^2+\delta^2)}}\right]^2\right\}^{-\frac{1}{2}}\end{aligned} \tag{19}$$

In turn, Eq. (19) after taking into account the equations (20)–(23)

$$\begin{cases}w=\dfrac{a^2}{b^2}<1\\ e=\sqrt{ab}\end{cases} \tag{20}$$

$$b=\frac{e}{\sqrt[4]{w}} \tag{21}$$

$$\frac{\delta}{b}=\frac{\delta}{e}\sqrt[4]{w} \tag{22}$$

$$\left(\frac{\delta}{b}\right)=\left(\frac{\delta}{e}\right)\sqrt{w} \tag{23}$$

we can transform it into Eq. (24) describing the thickness δ of the plastically deformed layer by the contact parameters $F(R_e e^2)^{-1}=f(w,\delta e^{-1})$

$$\frac{F}{R_e e^2}=\frac{\sqrt{2}}{3}\pi\frac{1-w}{\sqrt{w}}\left\{\left[\frac{\delta}{e}\sqrt[4]{w}(1-\nu)\left(\frac{1+w}{w}E(\varphi,k)-2F(\varphi,k)\right)+1-2\nu\right.\right.$$
$$\left.-\frac{w(1+w)(1-2\nu)-2\left(\frac{\delta}{e}\right)^2\sqrt{w}(\nu(1+w)-1)}{2w\sqrt{\left(w+\left(\frac{\delta}{e}\right)^2\sqrt{w}\right)\left(1+\left(\frac{\delta}{e}\right)^2\sqrt{w}\right)}}\right]^2$$
$$+\left[\frac{\delta}{e}\sqrt[4]{w}\left(\frac{\nu-w}{w}E(\varphi,k)+(1-\nu)F(\varphi,k)\right)+\frac{1-2\nu}{2}\right.$$
$$\left.+\frac{w\left(1+\left(\frac{\delta}{e}\right)^2\sqrt{w}\right)-2\nu\left(w+\left(\frac{\delta}{e}\right)^2\sqrt{w}\right)}{2w\sqrt{\left(w+\left(\frac{\delta}{e}\right)^2\sqrt{w}\right)\left(1+\left(\frac{\delta}{e}\right)^2\sqrt{w}\right)}}\right]^2 \tag{24}$$
$$+\left[\frac{\delta}{e}\sqrt[4]{w}\left(\frac{1-w\nu}{w}E(\varphi,k)-(1-\nu)F(\varphi,k)\right)+\frac{1-2\nu}{2}\right.$$
$$\left.\left.+\frac{w^2(2\nu-1)\left(\frac{\delta}{e}\right)^2\sqrt{w}(2(w\nu-1)+w)}{2w\sqrt{\left(w+\left(\frac{\delta}{e}\right)^2\sqrt{w}\right)\left(1+\left(\frac{\delta}{e}\right)^2\sqrt{w}\right)}}\right]^2\right\}^{-\frac{1}{2}}$$

here

$$E(\varphi,k)=arcctg\left(\frac{\delta}{e}\sqrt[4]{w}\right)\left(1-\frac{1}{4}(1-w)-\frac{3}{64}(1-w)^2\right)$$
$$+\frac{\delta}{e}\sqrt[4]{w}\frac{1}{1+\left(\frac{\delta}{e}\right)^2\sqrt{w}}\left[\frac{1}{4}(1-w)+\frac{3}{64}(1-w)^2+\frac{1}{32}(1-w)^2\frac{1}{1+\left(\frac{\delta}{e}\right)^2\sqrt{w}}\right] \tag{25}$$

$$F(\varphi,k)=arcctg\left(\frac{\delta}{e}\sqrt[4]{w}\right)\left(1-\frac{1}{4}(1-w)-\frac{8}{64}(1-w)^2\right)$$
$$+\frac{\delta}{e}\sqrt[4]{w}\frac{1}{1+\left(\frac{\delta}{e}\right)^2\sqrt{w}}\left[\frac{1}{4}(1-w)+\frac{9}{64}(1-w)^2+\frac{3}{32}(1-w)^2\frac{1}{1+\left(\frac{\delta}{e}\right)^2\sqrt{w}}\right] \tag{26}$$

where F is contact force; R_e is yield stress of the deformed material; ν is Poisson's ratio; E is Young's modulus; $= e=\sqrt{a\cdot b}$ is equivalent semi-axis of the contact ellipse (Hertzian semi-axis); a and b are minor and major semi-axis of the contact ellipse (Fig. 3), respectively; $w=a^2b^2<1$ is dimensionless auxiliary coefficient.

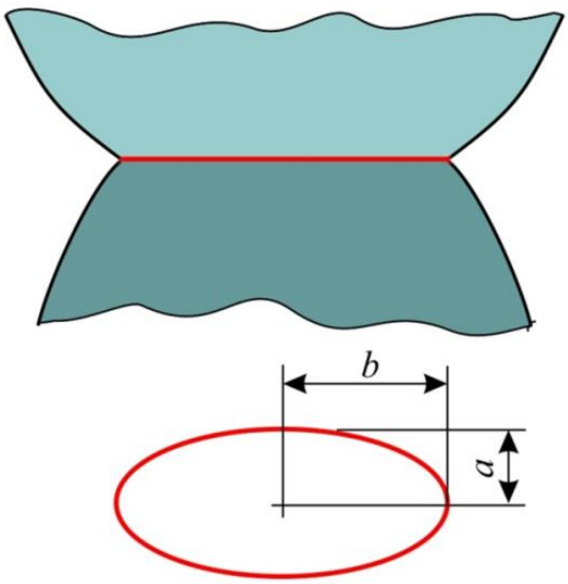

Fig. 3. Hertzian contact ellipse.

This equation concerns the general solution for the asymmetric stress state and was described by Mazur (2003). The solution to equation (24) for the case $a < b$ is a pencil of curves (each curve for a different value of w).

3. Results

Analytical calculations of the depth of the plastically deformed top layer were performed in the MathCAD program according to Eq. (24). The following data were assumed: diameter of the burnishing ball D = 6.25 mm, shaft diameter d = 48 mm, yield stress of shaft material R_e = 450 and R_e = 900 MPa, Young's modulus $E = 2.1\times10^5$ MPa and Poisson's ratio $\nu = 0.3$.

The results of contact force calculations using the asymmetric method were compared with the results obtained according to the classical (symmetric) solution (Jezierski, 1972) (Eq. (27)).

$$\frac{F}{R_e e^2} = \frac{4\pi}{3}\left[\frac{3}{1+\left(\frac{\delta}{e}\right)^2} + 2(1+\nu)\left(\frac{\delta}{e}arcctg\frac{\delta}{e} - 1\right)\right] \tag{27}$$

Results of numerical calculations of the contact forces and dimensions of half-axis of the contact ellipse obtained from the asymmetric and classical (symmetric) solutions are listed in Tables 1 and 2. The difference between the contact force values calculated using the asymmetric and symmetric solutions is 0.04–0.15% (Table 1) and 0.07–0.20% (Table 2), respectively. The difference between the values $e = a + b$ for both solutions does not exceed 0.11%. This is the result of the fact that the trace of the impression of a small diameter ball on the surface of a cylindrical roller is close to a circle (a ~ b). Figures 4a and 4b graphically present the influence of the depth of the plastically deformed top layer on the contact force for the yield stress of the roller material R_e = 450 MPa and R_e = 900 MPa, respectively. Approximation of the data points showed a power-law relationship between the depth of the plastically deformed top layer and the contact force.

Table 1. Results of numerical calculations of the contact forces and dimensions of half-axis of the contact ellipse obtained from the solution of the asymmetric case and the classical solution for a material with a yield strength of R_e = 450 MPa.

δ, mm	**Asymmetric case**				**Classical solution**	
	F, N	*a*, mm	*b*, mm	*e*, mm	*F*, N	*e* = *a* + *b*, mm
0.1	13.07	0.060	0.066	0.06296	13.05	0.06291
0/2	44.83	0.091	0.099	0.09495	44.80	0.09489
0.3	95.11	0.117	0.127	0.12200	95.04	0.12193
0.4	163.69	0.140	0.152	0.14621	163.60	0.14612
0.5	250.47	0.162	0.175	0.16848	250.35	0.16839

Table 2. Results of numerical calculations of the contact forces and dimensions of half-axis of the contact ellipse obtained from the solution of the asymmetric case and the classical solution for a material with a yield strength of R_e = 900 MPa.

δ, mm	Asymmetric case				Classical solution	
	F, N	a, mm	b, mm	e, mm	F, N	$e = a + b$, mm
0.1	34.23	0.083	0.090	0.08679	34.16	0.08669
0/2	104.58	0.121	0.131	0.12593	104.44	0.12582
0.3	212.96	0.153	0.166	0.15961	212.74	0.15949
0.4	358.68	0.182	0.198	0.18991	358.37	0.18977
0.5	541.38	0.209	0.227	0.21784	540.97	0.21770

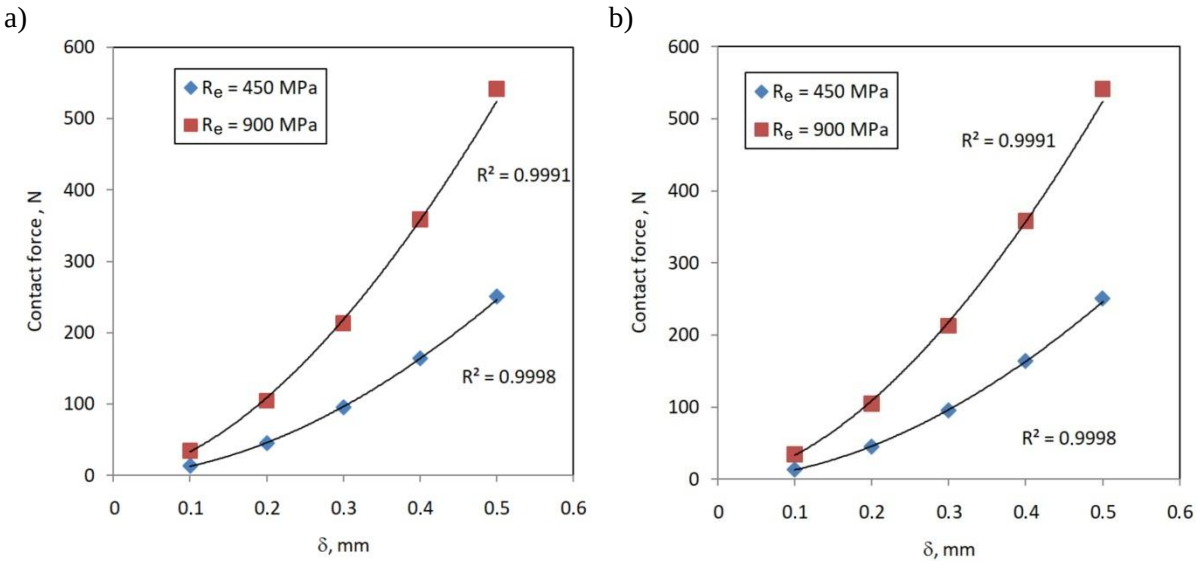

Fig. 4. Graphs of the relationship $F = f(\delta)$ obtained using the a) asymmetric and b) classical solution.

4. Conclusions

The depths of the plastically deformed top layer when burnishing with a small diameter ball (D < 20 mm) and in the range of low contact forces, calculated using the asymmetric and classical solutions, are similar to each other. The difference in the burnishing force value determined using both methods does not exceed 0.2%. From the geometric point of view, the trace of the ball impression on the shaft has similar values of the semi-axis $a \sim b$. Therefore, for small values of the ball diameter, both methods provide similar results. The relationship between the depth of the plastically deformed top layer and the contact force with an accuracy of $R^2 > 0.999$ can be presented using a power equation in the form $F = u \times \delta^h$, where u and h are constants.

References

Belyaev, N. M. (1957). *Trudy po teorii uprugosti i plasticznosti* [*Works on the theory of elasticity and plasticity*]. Maszgiz.

Chodor, J., & Kukielka, L. (2014). Using nonlinear contact mechanics in process of tool edge movement on deformable body to analysis of cutting and sliding burnishing processes. *Applied Mechanics and Materials 474*, 339–344. https://doi.org/10.4028/www.scientific.net/AMM.474.339

Czechowski, K., & Kalisz, J. (2015). Wybrane aspekty procesu nagniatania [Selected aspects of the burnishing process]. *Mechanik, 5-6*, 452–455. https://doi.org/10.17814/mechanik.2015.5-6.203

Czechowski, K., & Toboła, D. (2017). Gładkościowe nagniatanie ślizgowe stopów metali i kompozytów na osnowie metalowej [Slide finishing burnishing of metal alloys and metal matrix composites]. *Mechanik, 7*, 552–554. http://dx.doi.org/doi.org/10.17814/mechanik.2017.7.70

Dobrzyński, M., Javorek, L., Orłowski, K. A., & Przybylski, W. (2019). The effect of an active force while slide diamond burnishing of wooden shafts upon process quality. *Journal of Construction and Maintenance, 1*(112), 7–15.

Dyl, T. (2010). Wpływ nagniatania na umocnienie elementów części maszyn okrętowych [The influence of burnishing on the surface layer strengthening ship machine]. *Zeszyty Naukowe Akademii Morskiej w Gdyni, 64*, 36–42.

Dyl, T. (2011). Nagniatanie powierzchni płaskich elementów części maszyn okrętowych [The burnishing flat surfaces of machine parts ship]. *Zeszyty Naukowe Akademii Morskiej w Gdyni, 71*, 2011, 38–48.

Dzierwa, A., Gałda, L., Tupaj, M., & Dudek, K. (2020). Investigation of wear resistance of selected materials after slide burnishing process. *Eksploatacja i Niezawodność-Maintenance and Reliability, 22*(3), 432–439. https://doi.org/10.17531/ein.2020.3.5

Gałda, L., & Pająk, D. (2022). Analysis of the application of SIC ceramics as a tool material in the slide burnishing process. *Technologia i Automatyzacja Montażu*, *1*, 45–57. http://dx.doi.org/10.7862/tiam.2022.1.5

Huber, M. T. (1904). Właściwa praca odkształcenia jako miara wytężenia materiału [Specific work of strain as a measure of material effort]. *Czasopismo Techniczne*, *22*, 38–50, 61–62, 80–81.

Jezierski, J. (1972). *Obróbka maszynowa części maszyn zgniotem na zimno* [*Work hardening of machine parts*]. Prace Naukowe - Politechnika Warszawska: Mechanika, 19.

Jezierski, J., & Mazur, T. (2002). Analysis of the thickness of the plasticized zone in the surface burnishing process. *Archive of Mechanical Engineering*, *49*(2), 105–126.

Kaldunski, P., Patyk, R., Kukielka, L., Bohdal, L., Chodor, J., & Kulakowska, A. (2019). Numerical analysis and experimental researches of the influence of technological parameters burnishing rolling process on fatigue wear of shafts, *AIP Conference Proceedings*, *2078*, Article 020082. https://doi.org/10.1063/1.5092085

Kułakowska, A., Patyk, R., & Bohdal Ł. (2014). Zastosowanie obróbki nagniataniem w tworzeniu ekologicznego produktu [Application of burnishing process in creating environmental product]. *Annual Set The Environment Protection*, *16*, 323–335.

Mazur, T. (2003). Badania grubości warstwy wierzchniej odkształconej plastycznie po nagniataniu powierzchniowym [Testing the thickness of the plastically deformed surface layer after surface burnishing], [Unpublished doctoral dissertation]. Politechnika Radomska

Patyk, R., Kułakowska, A., & Nagnajewicz, S. (2017). Badanie wpływu głębokości nagniatania na chropowatość powierzchni wałków stalowych [Researches of the influence of burnishing depth on the surface roughness parameters of the steel shafts]. *Autobusy*, *12*, 1208–1211.

Przybylski W. (1987). *Technologia obróbki nagniataniem* [*Burnishing technology*]. Wydawnictwa Naukowo-Techniczne.

Przybylski, W. (2004). Nagniatanie stali o różnej twardosci narzędziami ceramicznymi [Burnishing of steel of various hardness with ceramic tools]. *Zeszyty Naukowe Politechniki Koszalińskiej*, *34*, 251–258.

Przybylski, W. (2016). Sliding burnishing technology of holes in hardened steel. *Advances in Manufacturing Science and Technology*, *40*(3), 43–51. https://doi.org/10.2478/amst-2016-001

Ryzyk, L. M., & Gradsztejn, I. S. (1964). *Tablice całek, sum, szeregów i iloczynów* [*Tables of integrals, sums, series and products*]. Wydawnictwo Naukowe PWN.

Sachin, B., Rao, C. M., Naik, G. M., & Puneet, N. P. (2021). Influence of slide burnishing process on the surface characteristics of precipitation hardenable steel. *SN Applied Sciences*, *3*, Article 223. https://doi.org/10.1007/s42452-021-04260-w

Skoczylas, A., & Zaleski, K. (2022). Study on the surface layer properties and fatigue life of a workpiece machined by centrifugal shot peening and burnishing. *Materials*, *15*, Article 6677. https://doi.org/10.3390/ma15196677

Zaleski, K. (2018). *Technologia nagniatania dynamicznego* [*Dynamic burnishing technology*]. Wydawnictwo Politechniki Lubelskiej.

Zaleski, K., & Skoczylas, A. (2019). Effect of slide burnishing on the surface layer and fatigue life of titanium alloy parts. *Advances in Materials Science*, *19*(4), 35–45. https://doi.org/10.2478/adms-2019-0020

Ocena Głębokości Warstwy Odkształconej Plastycznie w Procesie Nagniatania Wału za Pomocą Nagniataka Ceramicznego

Streszczenie

Nagniatanie jest jedną z najbardziej efektywnych metod poprawy wytrzymałości warstwy wierzchniej wałów w efekcie umocnienia odkształceniowego materiału. W tym artykule przedstawiono teoretyczne podejście do określania grubości warstwy wierzchniej odkształconej plastycznie na podstawie teorii Bielajewa. Założono kontakt dwóch ciał z niesymetrycznym stanem naprężenia. Rozważano również rozwiązanie klasyczne. Celem badań było porównanie obliczonych wartości grubości warstwy odkształconej plastycznie wyznaczonych za pomocą tych dwóch metod. W obliczeniach rozważono nagniatanie wałów o średnicy 48 mm wykonanych ze stali o granicy plastyczności R_e = 450 MPa oraz R_e = 900 MPa. Do nagniatania wykorzystano nagniatak z końcówką ceramiczną Si_3N_4. Stwierdzono, że w zakresie małych sił nacisku obliczone wartości grubości warstwy umocnionej za pomocą rozwiązania niesymetrycznego i metodą klasyczną są zbliżone. Stwierdzono również, że zależność pomiędzy głębokością odkształconej plastycznie warstwy wierzchniej a siłą nacisku można wyjaśnić równaniem potęgowym z dokładnością $R^2 > 0{,}999$.

Słowa kluczowe: nagniatanie, warstwa odkształcona plastycznie, teoria Bielajewa, wały